Neuropathology 2006; **26**, 43–49 doi:10.1111/j.1440-1789.2006.00654.x

Original Article

Brain stem lesions in sporadic Creutzfeldt–Jakob disease: A histopathological and immunohistochemical study

Masayuki Shintaku,[1] Chikao Yutani[2] and Katsumi Doh-ura[3]

[1]Department of Pathology, Osaka Red Cross Hospital, Tennoji, Osaka, [2]Department of Life Science, Faculty of Science, Okayama University of Science, Okayama, and [3]Department of Prion Research, Tohoku University Graduate School of Medicine, Aoba, Sendai, Japan

Lesions of the brain stem in sporadic CJD were histopathologically and immunohistochemically investigated using an anti-PrP antibody on ten consecutive autopsy cases. Three major histopathological changes, spongiform changes, neuronal loss and hypertrophic astrocytosis, were employed as parameters of the alterations. The quadrigeminal plate and pontine nuclei were the most severely and consistently affected structures, and immunoreactivity against PrP was seen in these structures. There existed some discrepancies between the severity of the lesions and the intensity of the immunoreactivity against PrP. The medulla oblongata essentially remained normal on histopathological examination, but the inferior olivary nucleus showed prominent PrP deposition. Although the general view that pathological alterations in the brain stem are relatively mild in sporadic CJD was confirmed in this study, lesions of variable degrees which might influence a patient's clinical course were still observed in many structures in the brain stem.

Key words: brain stem, CJD, histopathology, immunohistochemistry, PrP.

INTRODUCTION

The principal neuropathological features seen in a brain affected by sporadic CJD include spongiform changes of the neuropil, loss of neurons, proliferation of hypertrophic astrocytes and, in a subset of cases, the formation of amyloid plaque.[1,2] These changes are most prominent in the neocortex of the cerebrum and are also found in various degrees in the basal ganglia and thalamus. In many cases, the cerebellar cortex is also severely affected and, especially in the panencephalopathic type, the white matter of the cerebrum exhibits remarkable pathological alterations.[3] On the other hand, it is believed that pathological alterations in the brain stem below the level of the mesencephalon are mild in sporadic CJD, although involvement of the pontine base or inferior olivary nucleus has been occasionally described.[1,3–5] This is in contrast to other human prion diseases, such as kuru,[6,7] and also prion diseases of animals, such as scrapie,[8] and bovine spongiform encephalopathy (BSE),[9] in which the brain stem is consistently and severely affected by similar pathological processes.

There exist few reports which detail brain stem lesions in sporadic CJD.[10] We investigated such lesions by histopathological and immunohistochemical methods using an anti-PrP antibody on consecutive autopsy cases of sporadic CJD.

MATERIALS AND METHODS

From the autopsy files of the departments of pathology of the Osaka Red Cross Hospital and the National Cardiovascular Center, ten consecutive autopsy cases of sporadic (non-familial and non-iatrogenic) CJD were retrieved. No case of the variant CJD[11,12] was investigated. A summary of the clinicopathological findings of these cases is presented in Table 1. Analysis of the *PrP* gene had been only performed for the recently autopsied cases (cases 8–10), and in all of these the gene was the wild type and codon 129 was homozygous for methionine.

In all cases, the brain had been routinely examined after formalin fixation. Representative sections taken from many regions of the cerebrum and cerebellum were

Correspondence: Masayuki Shintaku, MD, Department of Pathology, Osaka Red Cross Hospital, Tennoji, Osaka 543-8555, Japan. Email: masa-s@sings.jp

Received 28 March 2005; revised and accepted 30 June 2005.

Table 1 Clinicopathological findings of the cases studied

Case	Age (years)	Gender	Duration (months)	Brain weight (grams)	Prion typing
1	70	F	20	830	
2	77	F	7	1110	
3	59	M	24	850	
4	75	F	35	900	
5	66	M	45	860	
6	67	M	18	1010	
7	71	M	16	Unknown	
8	71	M	7	1140	MM1
9	61	F	7	900	MM1
10	56	F	16	790	MM1

reviewed, and the neuropathological diagnosis of sporadic CJD was confirmed. Each brain stem had been cut in planes vertical to the long axis in all cases, and tissue sections had been taken from four to six different levels extending from the rostral mesencephalon to the caudal medulla oblongata. Paraffin sections had then been stained with HE, luxol fast blue-periodic acid-Schiff, modified Bielschowsky, and Nissl stains. We evaluated the lesions of the gray matter of the brain stem employing the following three histopathological parameters:[1,2] (i) spongiform changes of the neuropil; (ii) loss of neurons; and (iii) the proliferation of hypertrophic astrocytes. Other specific pathological alterations were also recorded. Because there was a subtle difference in the examined levels of sections between the cases because of the retrospective nature of this study, only easily identifiable, distinct nuclear groups were selected for evaluation. Changes in the white matter of the brain stem were excluded, because they were considered to largely represent secondary alterations caused by lesions in the cerebral or cerebellar cortex.

In eight cases for which preserved paraffin blocks were available, sections were recut and immunohistochemical investigations were performed using a monoclonal antibody against PrP (clone 3F4, DakoCytomation, Glostrup, Denmark; 1:100) and by employing the Envision Plus detection system (DakoCytomation) after pretreatment of the sections by hydrolytic autoclaving in 1.5 mmol hydrochloric acid at 121°C for 10 min.[13] Paraffin sections of the medulla oblongata were available only for cases 7–10.

The severity of individual lesions and the intensity of the immunohistochemical reactions were evaluated using the four-tiers grading system: (–) absent or negative; (±) equivocal or very weakly positive; (+) definitely present or positive; and (++) severe or intensely positive.

RESULTS

For the overall neuropathological features of the cerebral hemispheres and the cerebellum, in all cases the brain showed gross atrophy, and the thinning of the cerebral cortex was marked. The cerebellum also exhibited severe cortical atrophy along with the marked depopulation of granule cells and thinning of the molecular layer. No amyloid plaque was observed in any case. The white matter of the cerebral hemispheres showed diffuse myelin pallor and axonal loss. In addition, peculiar, localized spongiform changes of the subcortical white matter, which is a characteristic of panencephalopathic type CJD,[3] were noted in cases 9 and 10.

On gross examination, the mesencephalon and pons showed diffuse atrophy of mild to moderate degree in every case, and the pontine base had lost its bulge on the ventral surface. On the other hand, the medulla oblongata appeared almost normal on macroscopic observation. A summary of the brain stem lesions is presented in Table 2.

Mesencephalon

The superior and inferior colliculi were the most distinctly and consistently affected sites among the structures present in the mesencephalon. Spongiform changes were seen chiefly in the superficial layers, and neuronal loss and astrocytosis were found diffusely throughout these structures (Fig. 1). The periaqueductal gray matter was also involved, but less distinctly than in the quadrigeminal plate, and neuronal loss was not apparent. In case 1, a few senile plaques were observed in this region. Neurons of the oculomotor nucleus were well preserved, but spongiform changes were noted in cases 9 and 10. Of special interest, multiple large vacuoles were occasionally found in the neuronal perikarya in the oculomotor nucleus of these two cases (Fig. 2). In another case (case 3), similar vacuoles in the perikarya were found in several pigmented neurons of the substantia nigra. Pathological alterations in the red nucleus and reticular formation were mild except for case 9, in which spongiform changes and astrocytosis were noted to a moderate degree. In the substantia nigra, neuronal loss to a mild degree was noted in the zona compacta in most cases. Spongiform changes were clearly observed in four cases, and a few "foamy spheroids" were

Table 2 Summary of the histopathological and immunohistochemical findings of the brain stem

		Case 1				Case 2			Case 3				Case 4				Case 5			
		SC	NL	AS	PrP	SC	NL	AS	SC	NL	AS	PrP	SC	NL	AS	PrP	SC	NL	AS	PrP
Mesencephalon	Superior colliculus	–	+	++	+	NE	NE	NE	–	±	++	–	NE	NE	NE	NE	+	±	+	+
	Inferior colliculus	NE	NE	NE	NE	+	±	+	NE	NE	NE	NE	NE	NE	NE	NE	NE	NE	NE	NE
	Periaqued. gray matter	–	–	+	±	+	–	–	–	–	+	–	NE	NE	NE	NE	±	–	±	+
	Oculomotor nucleus	–	–	+	–	±	–	–	–	–	–	–	NE	NE	NE	NE	±	–	±	±
	Red nucleus	–	–	+	–	NE	NE	NE	–	–	+	–	±	–	+	–	–	–	±	–
	Reticular formation	–	–	+	+	±	–	±	–	–	+	–	NE	NE	NE	NE	–	–	±	±
	Subst. nigra. Z. comp.	–	+	+	–	–	–	–	+	+	+	–	++	+	+	–	++	±	±	±
	Subst. nigra. Z. reticu.	–	+	+	–	–	–	–	+	+	+	–	NE	NE	NE	NE	++	±	±	–
Pons	Locus ceruleus	–	±	+	+	NE	NE	NE	NE	NE	NE	NE	±	±	±	–	–	–	–	+
	Raphe nucleus	–	–	–	+	NE	NE	NE	–	–	+	+	±	±	±	–	–	–	–	+
	Reticular formation	–	–	–	+	NE	NE	NE	–	–	–	+	–	–	+	–	–	–	–	+
	Pontine nuclei	–	++	++	+	–	–	–	–	+	++	+	–	++	++	–	++	++	++	±
Medulla oblongata	Nucl. N. hypogloss.	–	±	+	NE	–	–	–	–	–	±	NE	–	–	+	NE	–	–	±	NE
	Nucl. dors. n. trigem.	–	–	–	NE	NE	NE	NE	–	–	±	NE	–	–	+	NE	–	–	±	NE
	Nucl. tr. spin. n. trigem.	–	–	–	NE	–	–	–	–	–	±	NE	–	–	+	NE	–	–	±	NE
	Raphe nucleus	–	–	–	NE	NE	NE	NE	–	–	±	NE	–	–	–	NE	–	–	±	NE
	Reticular formation	–	–	±	NE	–	–	–	–	–	±	NE	–	–	+	NE	–	–	±	NE
	Olivary nucleus	–	–	+	NE	–	–	–	–	–	+	NE	–	+	+	NE	–	+	+	NE
	Nucl. fasc. poster.	–	–	±	NE	–	–	–	–	–	–	NE	–	–	+	NE	NE	NE	NE	NE

(continued)

		Case 6			Case 7				Case 8				Case 9				Case 10			
		SC	NL	AS	SC	NL	AS	PrP	SC	NL	AS	PrP	SC	NL	AS	PrP	SC	NL	AS	PrP
Mesencephalon	Superior colliculus	+	+	+	+	+	+	+	+	+	+	+	+	+	+	+	–	+	+	+
	Inferior colliculus	+	+	+	+	+	+	–	NE	NE	NE	NE	NE	NE	NE	NE	–	+	+	++
	Periaqued. gray matter	–	±	+	+	–	+	+	+	–	+	±	+	±	+	+	–	–	+	+
	Oculomotor nucleus	–	–	–	–	–	–	–	±	–	±	±	+	–	+	±	+	–	–	+
	Red nucleus	–	–	+	–	–	–	–	±	–	±	±	+	–	+	–	–	–	–	–
	Reticular formation	–	–	+	+	–	+	–	±	–	±	±	+	–	+	±	±	–	±	+
	Subst. nigra. Z. comp.	–	+	–	–	+	±	–	±	+	+	±	–	–	±	+	+	±	±	+
	Subst. nigra. Z. reticu.	–	+	+	–	+	±	–	–	–	+	–	–	–	±	±	+	±	±	+
Pons	Locus ceruleus	–	–	–	–	–	–	–	±	–	±	+	–	–	±	+	–	–	–	+
	Raphe nucleus	–	–	–	–	–	–	+	–	–	–	+	+	±	+	±	–	–	–	+
	Reticular formation	–	–	–	–	–	–	+	±	–	±	+	+	–	+	±	–	–	–	+
	Pontine nuclei	–	+	+	–	+	+	±	±	+	+	+	±	±	+	+	+	++	++	+
Medulla oblongata	Nucl. N. hypogloss.	–	–	–	–	–	–	–	–	–	–	–	±	–	±	–	–	–	–	+
	Nucl. dors. n. trigem.	–	–	–	–	–	–	–	–	–	–	±	–	–	–	–	–	–	–	+
	Nucl. tr. spin. n. trigem.	–	–	–	–	–	–	–	–	–	–	±	+	–	+	–	–	–	–	+
	Raphe nucleus	–	–	–	–	–	–	–	–	–	–	±	±	–	±	–	–	–	–	+
	Reticular formation	–	–	–	–	–	–	–	–	–	±	±	+	–	+	+	–	–	+	+
	Olivary nucleus	–	+	+	–	+	+	+	–	+	+	+	+	+	+	+	–	–	+	++
	Nucl. fasc. poster.	–	–	–	–	–	–	–	–	–	+	–	+	–	+	–	–	–	–	++

AS, astrocytosis; NE, not examined; NL, neuronal loss; PrP, prion protein; SC, spongiform change.

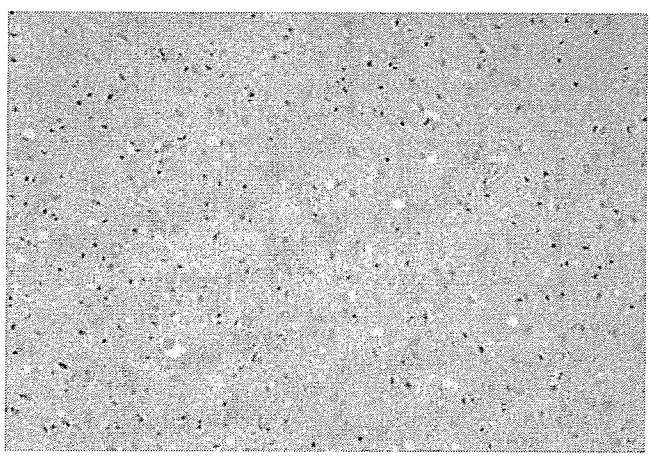

Fig. 1 Spongiform changes of moderate degree associated with neuronal loss and proliferation of hypertrophic astrocytes in the superior colliculus (case 8, HE stain).

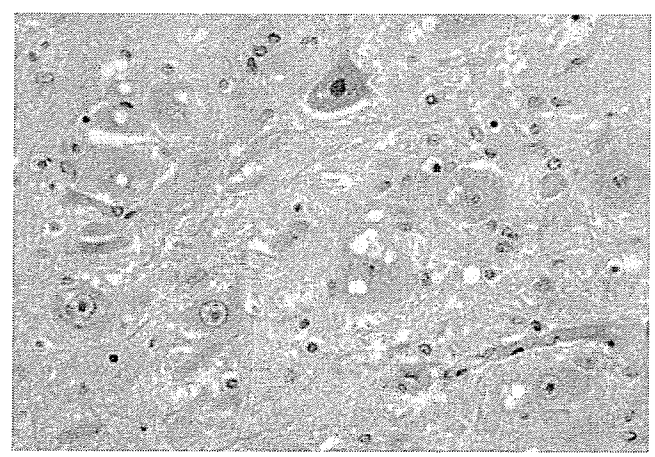

Fig. 2 Multiple large vacuoles found in the neuronal perikarya in the oculomotor nucleus (case 9, HE stain).

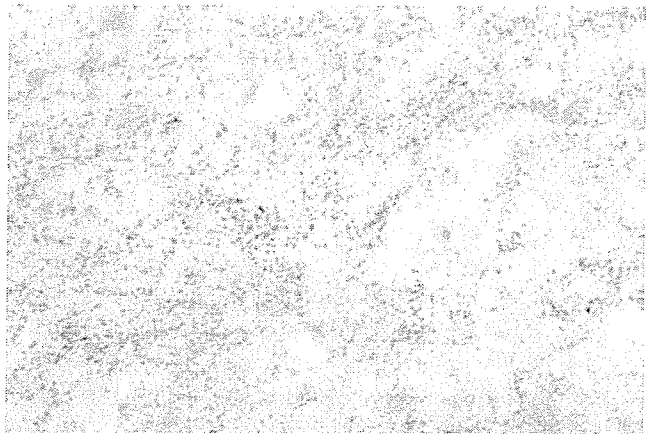

Fig. 3 Diffuse or synaptic type immunoreactivity against PrP in the neuropil of the superior colliculus (case 1, immunostain for PrP).

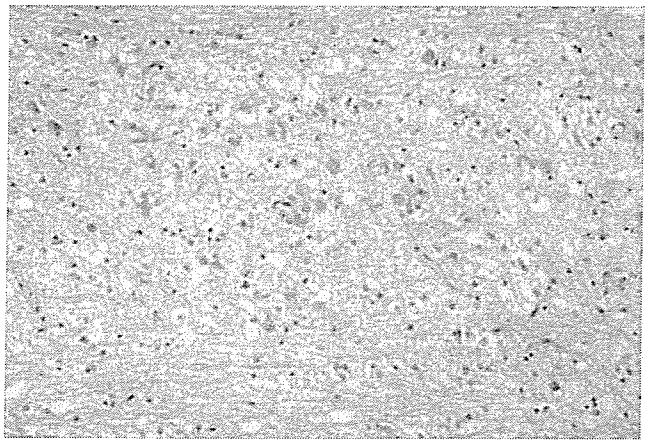

Fig. 4 Severe neuronal loss associated with spongiform changes and astrocytosis in the pontine nuclei. The sizes of the perikarya of the remaining neurons are reduced (case 10, HE stain).

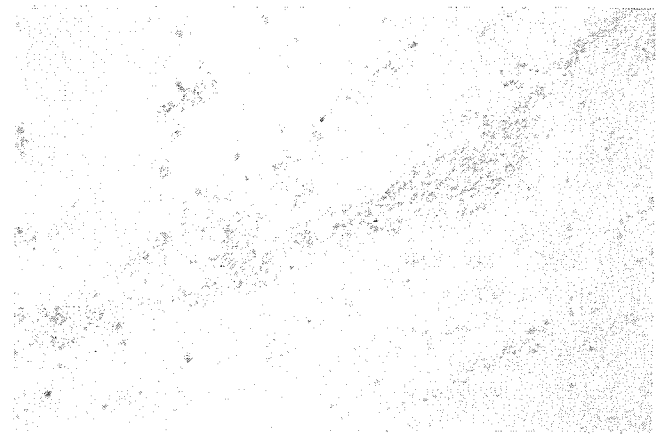

Fig. 5 Prominent deposition of PrP of diffuse or synaptic type in the pontine nuclei (case 8, immunostain for PrP).

Fig. 6 Neurons of the inferior olivary nucleus were well preserved, but marked deposition of PrP was found in the neuropil (case 10, immunostain for PrP).

occasionally found in the zona reticulata, showing mild astrocytosis.

Diffuse or synaptic-type immunoreactivity against PrP was consistently found in the quadrigeminal plate (Fig. 3), while it was weak or absent in other regions of the mesencephalon, and it roughly paralleled neuronal loss and astrocytosis.

Pons

The histopathological alterations in the pons were almost restricted to the pontine base except for case 9, and the tegmentum was well preserved as a whole. In case 9, spongiform changes accompanied by astrocytosis were seen in the reticular formation and raphe nucleus without apparent neuronal loss. The pontine base was affected in nine of the ten cases, and the loss of neurons of moderate to marked degree in association with hypertrophic astrocytosis was observed in the pontine nuclei (Fig. 4), while spongiform changes in the pontine nuclei were observed only in cases 5 and 10. The sizes of the perikarya of the remaining neurons in the pontine nuclei were reduced as a whole.

Diffuse or synaptic-type immunoreactivity against PrP was noted throughout all gray matter structures in the pons except in case 4, but was most prominent in the pontine nuclei (Fig. 5).

Medulla oblongata

The medulla oblongata was essentially histopathologically normal in all cases. In case 9, only mild spongiform changes accompanied by astrocytosis were noted throughout all

gray matter structures of the medulla oblongata, but no neuronal loss was observed in the tegmentum. The inferior olivary nucleus showed mild neuronal loss and astrocytosis in six cases, but these changes were considered most likely to be an age-related phenomenon and not of pathological nature. Axonal spheroids (dystrophic axon terminals) were consistently found in the gracile nucleus.

The results of anti-PrP immunohistochemistry, which was performed in four cases, were not anticipated based on the histopathological findings. Distinct, diffuse or synaptic-type immunoreactivity was noted throughout the inferior olivary nucleus in every case (Fig. 6). In addition, the tegmental structures showed diffuse immunoreactivity in case 10.

DISCUSSION

In sporadic CJD, the brain stem is comparatively spared from pathological alterations, and this is a characteristic of sporadic CJD,[1,4,5] a condition which is distinct from kuru[6,7] or prion diseases in animals such as scrapie[8] and BSE[9] in which the brain stem is severely affected. A previous western immunoblot analysis of the intracerebral distribution of infectious amyloid protein (PrP) in human spongiform encephalopathy revealed the almost complete absence of amyloid protein in the brain stem in sporadic CJD.[14] On the other hand, in variant CJD spongiform changes are occasionally found in the periaqueductal gray matter and pontine nuclei, and neuronal loss with astrocytosis can be seen in structures such as the superior and inferior colliculi, periaqueductal gray matter, inferior olivary nucleus and dorsal vagal nucleus.[12] It is unknown at present why this difference in the distribution of lesions occurs among various kinds of prion disease. In sporadic CJD, the brain stem is less vulnerable or resistant to lesions caused by PrP. It is therefore intriguing to observe in full detail the pathological alterations of the brain stem in sporadic CJD, because progression of the disease might be slower in the brain stem than in the cerebral or cerebellar cortex. By close observation of the brain stem lesions, we might be able to determine the pathological changes in the early stages of the disease.

The results obtained in the present study supported the general view that the brain stem lesions are of mild degree in sporadic CJD. However, on closer examination, some specific and non-specific lesions of variable degree were found at various sites, and this is a phenomenon which is similar with the lesions seen in the hippocampus in sporadic CJD.[15] We discuss some of the brain stem lesions observed and make brief comments on each topic below.

1 We adopted three histopathological parameters[1,2] to evaluate the brain stem lesions, spongiform changes of the neuropil, neuronal loss and hypertrophic astrocytosis, but they did not necessarily occur in parallel. While the proliferation of astrocytes was noted in almost all lesions, it did not accompany neuronal loss in some regions, and spongiform changes were not apparent in the brain stem in most cases except for in the quadrigeminal plate and substantia nigra. Whereas spongiform changes in CJD are generally regarded an early event which precedes neuronal loss and astrocytosis,[4] astrocytosis was observed to occur before the appearance of spongiform changes in experimentally transmitted scrapie.[16] The proliferation of hypertrophic astrocytes therefore might not simply be a secondary change. (It should be also noted that the intensity of immunoreactivity against PrP did not parallel the histopathological alterations. In many regions, for example the pontine tegmentum and inferior olivary nucleus, the deposition of PrP was noted without accompanying spongiform changes or neuronal loss. This might indicate that these brain stem structures are resistant to the pathological processes induced by PrP.)

2 In the mesencephalon, the superior and inferior colliculi are consistently vulnerable in sporadic CJD, and similar involvement of the quadrigeminal plate was previously noted by some authors.[4] While the substantia nigra was affected in most cases, the changes were relatively mild. A few senile plaques were found in the periaqueductal gray matter in one case (case 1). Although the occurrence of amyloid plaques with a wide morphological spectrum has been previously documented in the mesencephalon of some cases of sporadic CJD,[5] the plaques in our case were immunohistochemically negative for PrP and probably represented a senile change.

3 The formation of large vacuoles in the perikarya of neurons has previously been consistently observed in the brain stem, especially in the medulla oblongata, in BSE[9,17] and scrapie,[8] and is pathognomonic for these disorders. Perikaryal vacuole formation is not a prominent feature in the cerebral or cerebellar cortex in sporadic CJD. On the other hand, it is commonly observed in the brain stem in kuru.[6,7] In the present study, this was seen in the oculomotor nucleus in two cases and in the substantia nigra in another case, without being accompanied by neuronal loss.

4 In the pontine base, although spongiform changes of the neuropil were found in only two cases, neuronal loss with astrocytosis of moderate to marked degree was noted in the pontine nuclei in most. The deposition of PrP was also observed in five of eight cases. It is certain that the pontine nuclei are sites which are consistently affected by the pathological processes that occur in sporadic CJD, and this is in accordance with the observations of Tateishi *et al.*[5] Recently Iwasaki *et al.*[10] also described gross atrophy of the pontine base, neuronal loss and prominent PrP immunoreactivity in the pontine nuclei in most cases of sporadic CJD, and similar results were also obtained for variant CJD.[12]

The sizes of the perikarya of the remaining neurons in the pontine nuclei appeared to be generally reduced in our series. Because the sizes of the neuronal perikarya show considerable regional variation within the pontine nuclei,[18] a more strict quantitative study is needed to confirm this observation. Neurons of the pontine nuclei send their axons to the cerebellar granule cell layer and also receive many fibers from the broad regions of the cerebral cortex.[18] Therefore, the possibility is considered that the atrophy of the neuronal perikarya in the pontine nuclei was partly caused by anterograde and/or retrograde trans-synaptic degeneration, as suggested by Tateishi *et al.*[5]

5 The medulla oblongata was preserved in an approximately normal state histopathologically except for one case. In thalamic type of CJD, severe degeneration of the inferior olivary nucleus constantly occurs.[19,20] In the present series, no case of thalamic type CJD was included and degeneration of the inferior olivary nucleus was not noted. However, in spite of the absence of pathological neuronal loss, the deposition of PrP was consistently found in the inferior olivary nucleus.

In recent years, the variability of clinicopathological phenotypes in patients with sporadic CJD has been demonstrated to depend on a polymorphism at codon 129 of the *PrP* gene as well as a pattern on Western immunoblot analysis of PrP, and a new classification scheme based upon these data is widely being employed.[21] Because the present study is a retrospective one that was performed on archival autopsy materials, the results of molecular analysis of PrP and its gene were not available for most of the cases. This is a major limitation of our study, and an investigation for the correlation of the molecular characteristics of PrP and pathological findings of brain stem lesions in sporadic CJD should be performed in future studies. At this stage, very limited inference can be made on the genotypes of *PrP* in the present series. Judging from the fact that in more than 90% of the Japanese population codon 129 of the *PrP* gene is homozygous for methionine (MM type) and also judging from the clinicopathological features of each patient in our series (periodic synchronous discharge was observed on electroencephalogram in all patients), it is supposed that most of our cases 1–7 are probably the MM1 type.

The relationship between the histopathological and immunohistochemical findings of the brain stem and the duration of the clinical course is another problem that remains to be elucidated. In the present series, the severity of the histopathological findings and the regional distribution of the immunohistochemical reactivity of PrP varied from case to case, and we could not find a clear correlation between the duration of the clinical course and these findings in the brain stem lesions.

In summary, we showed that in sporadic CJD pathological alterations of variable degree were observed in the brain stem, in particular in the quadrigeminal plate and pontine nuclei, although spongiform changes were found only infrequently. The medulla oblongata did not show any significant histopathological lesions. The deposition of PrP was mainly observed in the quadrigeminal plate and pontine nuclei. We also noted this in the pontine tegmentum and inferior olivary nucleus, which appeared to be approximately normal by histopathological examination. The remaining problems include the relationships between these changes in the brain stem and the lesions in the cerebellum, the possibility of trans-synaptic degeneration of neurons in the pontine nuclei, the clinical significance of these brain stem lesions, and the reasons for the differences between the lesions of the brain stem in sporadic CJD and those in kuru or variant CJD.

REFERENCES

1. Budka H, Aguzzi A, Brown P *et al.* Neuropathological diagnostic criteria for Creutzfeldt-Jakob disease (CJD) and other human spongiform encephalopathies (prion diseases). *Brain Pathol* 1995; **5**: 459–466.
2. Ironside JW. Review. Creutzfeldt-Jakob disease. *Brain Pathol* 1996; **6**: 379–388.
3. Mizutani T, Okumura A, Oda M, Shiraki H. Panencephalopathic type of Creutzfeldt-Jakob disease. Primary involvement of the cerebral white matter. *J Neurol Neurosurg Psychiat* 1981; **44**: 103–115.
4. Masters CL, Richardson EP Jr. Subacute spongiform encephalopathy (Creutzfeldt-Jakob disease). The nature and progression of spongiform change. *Brain* 1978; **101**: 333–344.
5. Tateishi J, Sato Y, Ohta M. Creutzfeldt-Jakob disease in humans and laboratory animals. *Progr Neuropathol* 1983; **5**: 195–221.
6. Klatzo I, Gajdusek DC, Zigas V. Pathology of kuru. *Lab Invest* 1959; **8**: 799–847.
7. Hainfellner JA, Liberski PP, Guiroy DC *et al.* Pathology and immunocytochemistry of a kuru brain. *Brain Pathol* 1997; **7**: 547–553.
8. Wood JLN, McGill IS, Done SH, Bradley DR. Neuropathology of scrapie. A study of the distribution patterns of brain lesions in 222 cases of natural scrapie in sheep, 1982–1991. *Vet Rec* 1997; **140**: 167–174.
9. Wells GAH, Wilesmith JW. The neuropathology and epidemiology of bovine spongiform encephalopathy. *Brain Pathol* 1995; **5**: 91–103.
10. Iwasaki Y, Sobue G, Yoshida M, Hashizume Y. Neuropathological characteristics of brainstem lesions in sporadic Creutzfeldt-Jakob disease. *Brain Pathol* 2003; **13**: s149.

11. Will RG, Ironside JW, Zeidler M *et al.* A new variant of Creutzfeldt-Jakob disease in the UK. *Lancet* 1996; **347**: 921–925.
12. Ironside JW, Head MW, Bell JE, McCardle L, Will RG. Laboratory diagnosis of variant Creutzfeldt-Jakob disease. *Histopathol* 2000; **37**: 1–9.
13. Kitamoto T, Shin RW, Doh-ura K *et al.* Abnormal isoform of prion proteins accumulates in the synaptic structures of the central nervous system in patients with Creutzfeldt-Jakob disease. *Am J Pathol* 1992; **140**: 1285–1294.
14. Brown P, Kenney K, Little B *et al.* Intracerebral distribution of infectious amyloid protein in spongiform encephalopathy. *Ann Neurol* 1995; **38**: 245–253.
15. Mizusawa H, Hirano A, Llena JF. Involvement of hippocampus in Creutzfeldt-Jakob disease. *J Neurol Sci* 1987; **82**: 13–26.
16. Wiley CA, Burrrola PG, Buchmeier MJ *et al.* Immunogold localization of prion filaments in scrapie-infected hamster brains. *Lab Invest* 1987; **57**: 646–656.
17. Wells GAH, Hancock RD, Cooley WA, Richards MS, Higgins RJ, David GP. Bovine spongiform encephalopathy. Diagnostic significance of vacuolar changes in selected nuclei of the medulla oblongata. *Vet Rec* 1989; **125**: 521–524.
18. Carpenter MB, Sutin J. *Human Neuroanatomy*, 8th edn. Baltimore/London: Williams & Wilkins, 1983.
19. Mizusawa H, Ohkoshi N, Sasaki H, Kanazawa I, Nakanishi T. Degeneration of the thalamus and inferior olives associated with spongiform encephalopathy of the cerebral cortex. *Clin Neuropathol* 1988; **7**: 81–86.
20. Kornfeld M, Seelinger DF. Pure thalamic dementia with a single focus of spongiform change in cerebral cortex. *Clin Neuropathol* 1994; **13**: 77–81.
21. Parchi P, Castellani R, Capellari S *et al.* Molecular basis of phenotypic variability in sporadic Creutzfeldt-Jakob disease. *Ann Neurol* 1996; **39**: 767–778.

Neuropathology 2006; **26**, 82–88 doi:10.1111/j.1440-1789.2006.00638.x

Case Report

Increased asymmetric pulvinar magnetic resonance imaging signals in Creutzfeldt–Jakob disease with florid plaques following a cadaveric dura mater graft

Yoshinobu Wakisaka,[1,2] Naohiko Santa,[2,3] Katsumi Doh-ura,[4] Tetsuyuki Kitamoto,[4] Setsuro Ibayashi,[2] Mitsuo Iida[2] and Toru Iwaki[1]

[1]Department of Neuropathology, Neurological Institute, and [2]Department of Medicine and Clinical Science, Graduate School of Medical Sciences, Kyushu University, Fukuoka, [3]Cerebrovascular Department, Neuroscience Institute, St Mary Hospital, Kurume, and [4]Department of Prion Research, Tohoku University Graduate School of Medicine, Sendai, Japan

A 9-year-old Japanese girl received a cadaveric dura mater graft during surgery following a head injury with brain contusion. She continued to do well, but when she became 19-years-old, she gradually showed a violent character and was treated in a psychiatric hospital. Another 6 years later, 200 months after the procedure, she developed a progressive gait ataxia, which subsequently led to her death within 10 months of onset. An autopsy showed she had CJD. This patient represents an atypical case of dura-associated CJD (dCJD) with unusual clinicopathological features including the late occurrence of myoclonus, an absence of periodic synchronous discharges in the electroencephalogram, and the presence of widespread florid plaques. However, our detection of an asymmetrical increase in the MRI-derived images of pulvinar nuclei has not been previously observed in other atypical cases of dCJD. Because atypical dCJD cases share several clinicopathological features with those of vCJD, and because asymmetrical hyperintense signals in the pulvinar have been observed in some neuropathologically confirmed vCJD cases, we had some difficulty in a differential diagnosis between atypical dCJD and vCJD. This is the first atypical dCJD case showing a pulvinar high signal compared with all other basal ganglia on MRI.

Key words: CJD, dura graft, MRI, pulvinar sign, vCJD.

Correspondence: Dr Yoshinobu Wakisaka, MD, PhD, Department of Medicine and Clinical Science, Graduate School of Medical Sciences, Kyushu University, 3-1-1 Maidashi, Higashi-ku, Fukuoka, 812-8582, Japan. Email: w-yoshi@intmed2.med.kyushu-u.ac.jp

Received 21 January 2005; revised and accepted 11 April 2005.

INTRODUCTION

Most dura-associated CJD (dCJD) cases have similar clinicopathological features to sporadic CJD (sCJD), presenting progressive mental deterioration, ataxia, myoclonus and characteristic EEG findings such as periodic discharges.[1] However, some patients with atypical dCJD exhibit clinicopathological features distinct from those of most dCJD cases have some resemblance to vCJD cases; that is, a slow progressive clinical course with the absence or late occurrence of periodic discharges on EEG, and the presence of widespread florid plaques in addition to widespread spongiform change, neuronal loss and astrocytosis.[2–8] On the other hand, the radiological features are different between atypical dCJD and vCJD cases. While vCJD cases present pulvinar high signals compared to all other basal ganglia,[9,10] atypical dCJD cases have not been reported to show such hyperintensity in pulvinar nuclei.[2–8] Moreover, the pathological features of the pulvinar nuclei are also different between atypical dCJD and vCJD cases. Here, we report an atypical dCJD case presenting asymmetrical pulvinar hyperintensity on MRI with different pathological characteristics of the pulvinar nucleus from those of reported atypical dCJD and vCJD cases.

CLINICAL SUMMARY

In November 1985, a 9-year-old Japanese girl received a cadaveric dural graft (Lyodura, B Braun Melsungen AG, Germany) at left frontotemporal region following a head injury with brain contusion. Six months later, she had a seizure and anti-epileptic drugs were administered. However, she did not take anti-epileptic drugs regularly, and epilepsy

frequently occurred. From 1995, she gradually developed a violent character. She was diagnosed as suffering a post-traumatic psychosis and received treatment in a psychiatric hospital. In June 2002, 200 months after the procedure, she began to develop an ataxic gait and became bed-ridden. By January 2003, she gradually showed memory disturbance and lost her spontaneous speech and was unable to communicate. She also exhibited myoclonic jerks in her upper limbs. She frequently suffered from aspiration pneumonia, and was brought to our hospital for respiratory insufficiency on 9 April 2003. On admission, she was akinetic and mute with decorticate posturing. There was no apparent history of depression, anxiety, apathy or delusions. Neurological examination showed moderate rigidity in bilateral upper and lower extremities, and myoclonus in bilateral upper extremities. The light reflex, corneal reflex and oculocephalic reflex were all normal. The motor and sensory systems could not be examined in detail. Deep tendon reflexes were normal. There was slow activity without any periodic discharge in her EEG. One week before her death, T2-weighted and proton density-weighted brain MRI showed significant hyperintensity in the thalamic pulvinar nuclei, which was predominantly on the left side, and moderate hyperintensity of the basal ganglia (Fig. 1A,B). Diffusion-weighted and gadolinium(III)-diethyltriaminepentaacetic acid (Gd-DTPA)-enhanced MRI revealed hyperintense signals in the pulvinar (Fig. 1C,D). The brain MRI also presented hyperintense signal by T2-weighted and proton density-weighted images and hypointense signal by diffusion-weighted and Gd-DTPA-enhanced images at the left frontal lobe, corresponding to where the brain contusion existed. In addition, Gd-DTPA enhanced images revealed hyperintense signals at the margin of the brain contusion. Based on the findings of the brain MRI, the diagnosis of dCJD was suspected. However, her respiratory insufficiency progressively worsened and she developed septic shock. Therefore, we could not assess further examination including the cerebrospinal fluid level of the 14-3-3 protein. She died on 19 April, 2003, 10 months after the onset of ataxic gait. The patient's family gave informed consent for the genetic and postmortem studies.

PATHOLOGICAL FINDINGS, IMMUNOBLOTTING AND GENE ANALYSIS

On examination, her brain weighed 1120 g, and there was a large defect in the left basal forebrain. While cerebral atrophy was not obvious, there was substantial atrophy of the cerebellum. The right side of the half-brain was deep-frozen for biochemical examination, and the other half was fixed in buffered formalin. Microscopically, most cerebral cortices had mild to moderate spongiform changes, neuronal loss, and astrocytosis with a predilection for the deep cortical layers. In contrast, the cingulate gyrus and insular cortex exhibited moderate to severe pathological changes throughout the whole layers. The putamen showed moderate spongiform change, neuronal loss and astrocytosis. Anterior nucleus of the thalamus presented mild spongiform change and neuronal loss, and moderate astrocytosis. Ventral lateral nucleus and dorsomedial nucleus of the thalamus displayed mild spongiform change, moderate neuronal loss and astrocytosis. Pulvinar nucleus of the thalamus exhibited the most severe neuronal loss and spongiform change, and greater astrocytosis than the cerebral cortices (Table 1). The hippocampus was almost completely spared. In the cerebellum, moderate atrophy of the molecular layer was associated with mild spongiform change and astrocytosis, while moderate neuronal loss of the granule layer and severe neuronal loss of the dentate nucleus was associated with moderate astrocytosis. The Purkinje cells were almost completely preserved. In HE sections, we frequently noted Kuru plaques in a number of regions of the cerebral cortex, the putamen and the pulvinar nucleus of the thalamus. The cores of the plaques were stained with PAS, and, when stained with Congo red, appeared apple green in polarized light. In addition, many of the Kuru plaques were surrounded by a zone of vacuolar change, consistent with florid plaques, which are known hallmarks of vCJD. Although the pulvinar nucleus of the thalamus presented frequent Kuru plaques, there were only a few plaques in anterior, ventral lateral and dorsomedial nuclei of the thalamus. Immunohistochemistry for PrP revealed widespread synaptic staining and numerous plaque-like deposits, including florid plaques in all areas of the cerebral cortices, putamen, pulvinar nucleus of the thalamus and white matter of the cerebellum. The globus pallidus, the anterior, ventral lateral and dorsomedial nuclei of the thalamus, and molecular layer of the cerebellum mainly showed synaptic staining associated with mild granular prion protein depositions. In addition, there were PrP deposits surrounding blood vessels, neuronal cell bodies and processes in the cerebral cortex and in the pulvinar nucleus (Fig. 2). The region around the head injury with brain contusion showed mild spongiform change with severe astrocytosis. Only a few Kuru plaques were found in this region (Table 1).

The sequence analysis of prion protein gene (*PRNP*) derived from the brain tissue showed no mutation with homozygous for methionine at codon 129 or for glutamate at codon 219, which are polymorphic sites of the *PrP* gene. Immunoblotting for the abnormal prion protein in the brain demonstrated a type 1 prion protein glycoform pattern (Parchi's classification)[11] (Fig. 3). The final diagnosis was atypical dCJD.

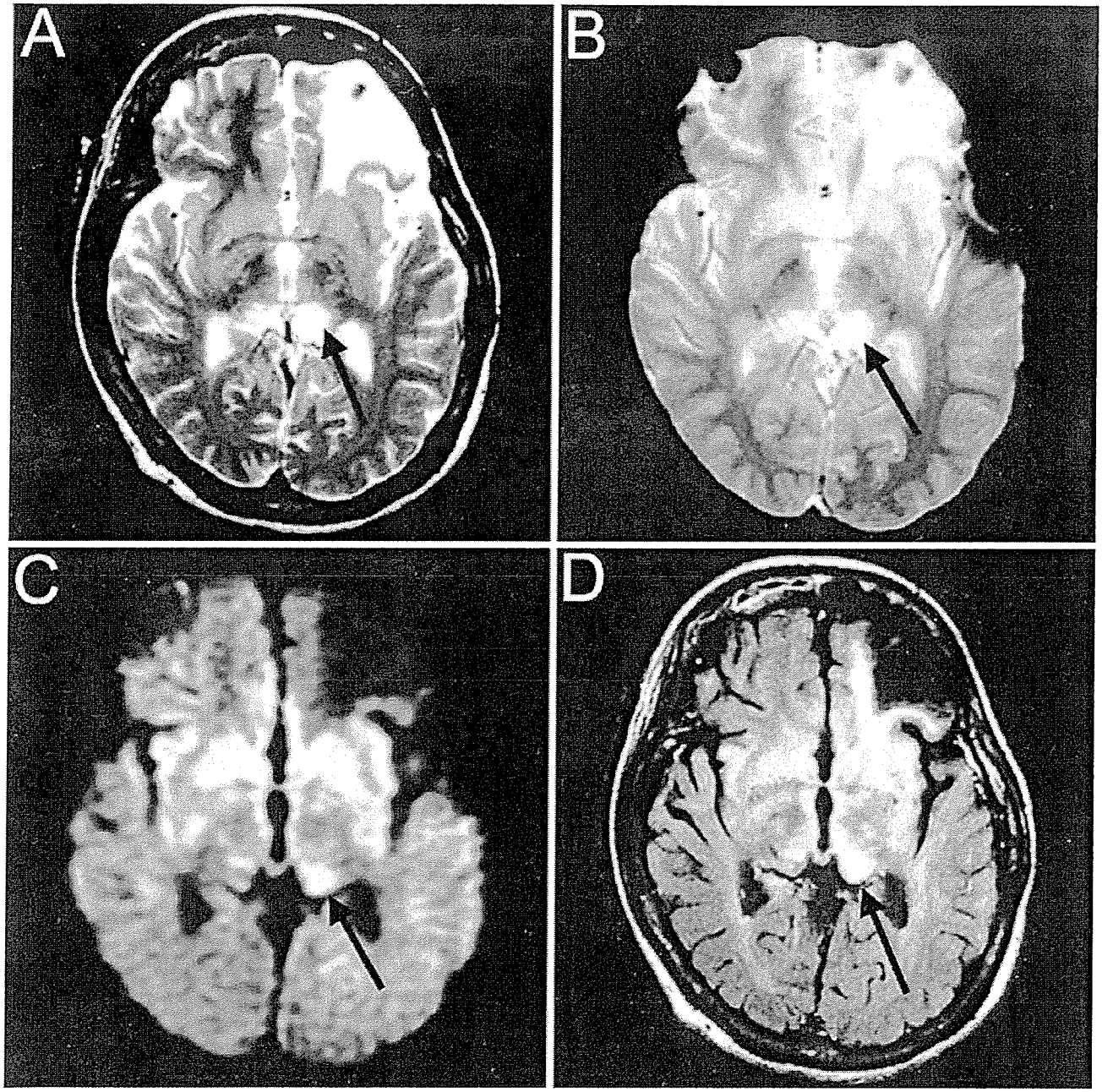

Fig. 1 Neuroradiological images. (A) T2-weighted image, (B) proton density-weighted image, (C) diffusion-weighted image, and (D) gadolinium(III)-diethyltriaminepentaacetic acid (Gd-DTPA)-enhanced brain MRI obtained 1 week prior to death. The images reveal hyperintensity in the pulvinar of the thalamus, and is more apparent in the left side (arrows). Images also show intense bilateral signals in the caudate nuclei and putamen.

DISCUSSION

We present the first atypical dCJD case to show a high pulvinar signal compared with all other basal ganglia on MRI, prominent lesions with severe spongiform changes, neuronal loss and numerous florid plaques in the posterior thalamus at autopsy.

Most dCJD cases take the form of typical sCJD.[1] Most dCJD cases are clinically evident as a progressive mental deterioration, ataxia and myoclonus. Periodic discharges

are often noted in the EEG before the terminal stage of the clinical course. The disease often progresses rapidly and the clinical course lasts less than 2 years. MRI of dCJD cases has previously shown either normal or non-specific and diffuse brain atrophy.[12] T2-weighted MRI has also shown sCJD cases frequently exhibit symmetrical and hyperintense changes in the putamen and caudate head compared with the thalamus and cerebral cortex.[13,14] In cases of sCJD, high-intensity signals in the cerebral and cerebellar cortex are also occasionally seen in fluid-attenuated inversion recovery, proton density-weighted and diffusion-weighted MRI-derived images.[13] Pathologically, the cerebral cortex and cerebellum of dCJD cases are substantially affected. Severe spongiform changes, astrocytosis and neuronal loss are found throughout the brain and cause substantial atrophy, resulting in brain weights of less than 1000 g. Immunohistochemistry reveals diffuse synaptic type deposition of PrP. None or few amyloid plaques are found in the brain.

However, among more than 110 alleged dCJD cases,[15] there have been some atypical dCJD patients with clinicopathological features which are different from those of sCJD and most dCJD cases but share several features with those of vCJD.[2–8] These atypical dCJD and vCJD cases show a slowly progressive clinical course reaching the state of akinetic mutism. The reported duration of atypical dCJD were ranged 5–24 months.[2–8] This duration resembled cases of vCJD, whose duration ranged 8–38 months.[16] In addition, periodic discharges on EEG were commonly absent in both atypical dCJD and vCJD cases. On the other hand, there are several different clinical features between these cases. While most atypical dCJD cases present initially with ataxia and mental deterioration, such as disorientation or memory disturbance often following the ataxia,[2–8] many vCJD cases initially suffer from sensory symptoms including persistent limb pain and/or persistent psychiatric symptoms as depression, anxiety, apathy and withdrawal.[16] Ataxia was reported to develop about 6 months after the onset of psychiatric and sensory symptoms.[16] Moreover, although myoclonus is absent or occurred at the end stage of the disease in atypical dCJD cases, involuntary movements including myoclonus are commonly noted during the clinical course of vCJD cases.[16] The duration of the disease of our case and the absence of periodic discharges on EEG were similar to those features of atypical dCJD and vCJD cases. On the other hand, because our case presented progressive cognitive impairment after the onset of ataxia, and because myoclonus was absent until the end stage of the disease, the clinical course of our case more resembled those of atypical dCJD than vCJD cases.

Pathologically, most atypical dCJD and vCJD cases show widespread spongiform change, neuronal loss and astrocytosis. These pathological changes are mild in the cerebral cortex and severe in caudate nucleus, putamen and cerebellum in both atypical dCJD and vCJD cases.[2–8]

Table 1 Neuropathological findings of left side of the half brain

	Spongiform change	Neuronal loss	Astrocytosis	Kuru plaques
MFG	+++	+	++	+++
MTG	+	+	++	++
IPG	+	+	++	+
PVC	+	+	+	++
Cingulate gyrus	+++	++	++	++
Insular cortex	++	++	++	+++
Hippocampus	–	–	–	–
Globus pallidus	+	+	+	–
Putamen	++	++	++	++
Thalamus AN	+	+	++	+
DMN	+	++	++	+
VLN	+	++	++	+
PN	+++	+++	+++	+++
Contusion area	+		+++	+
Cerebellum ML	+		+	–
PCL		–		
GL		++	++	
WM			++	+
DN		+++	++	–

MFG, middle frontal gyrus; MTG, middle temporal gyrus; IPG, Inferior parietal gyrus; PVC, primary visual cortex of occipital lobe; AN, anterior nucleus; DMN, dorsomedial neucleus; VLN, ventral lateral nucleus; PN, pulvinar nucleus; ML, molecular layer; PCL, purkinje cell layer; GL, granular layer; WM, white matter; DN, dentate nucleus.

Spongiform change and neuronal loss are absent (–), mild (+), moderate (++), severe (+++) on HE sections. Astrocytosis and Kuru plaques are absent (–), mild (+), moderate (++), severe (+++) on sections of immunohistochemistry probed with an anti-GFAP antibody (polyclonal, DAKO, Glostrup, Denmark) and antiprion protein antibody (monoclonal, clone 3F4, Senetek, Maryland Heights, MO, USA), respectively.

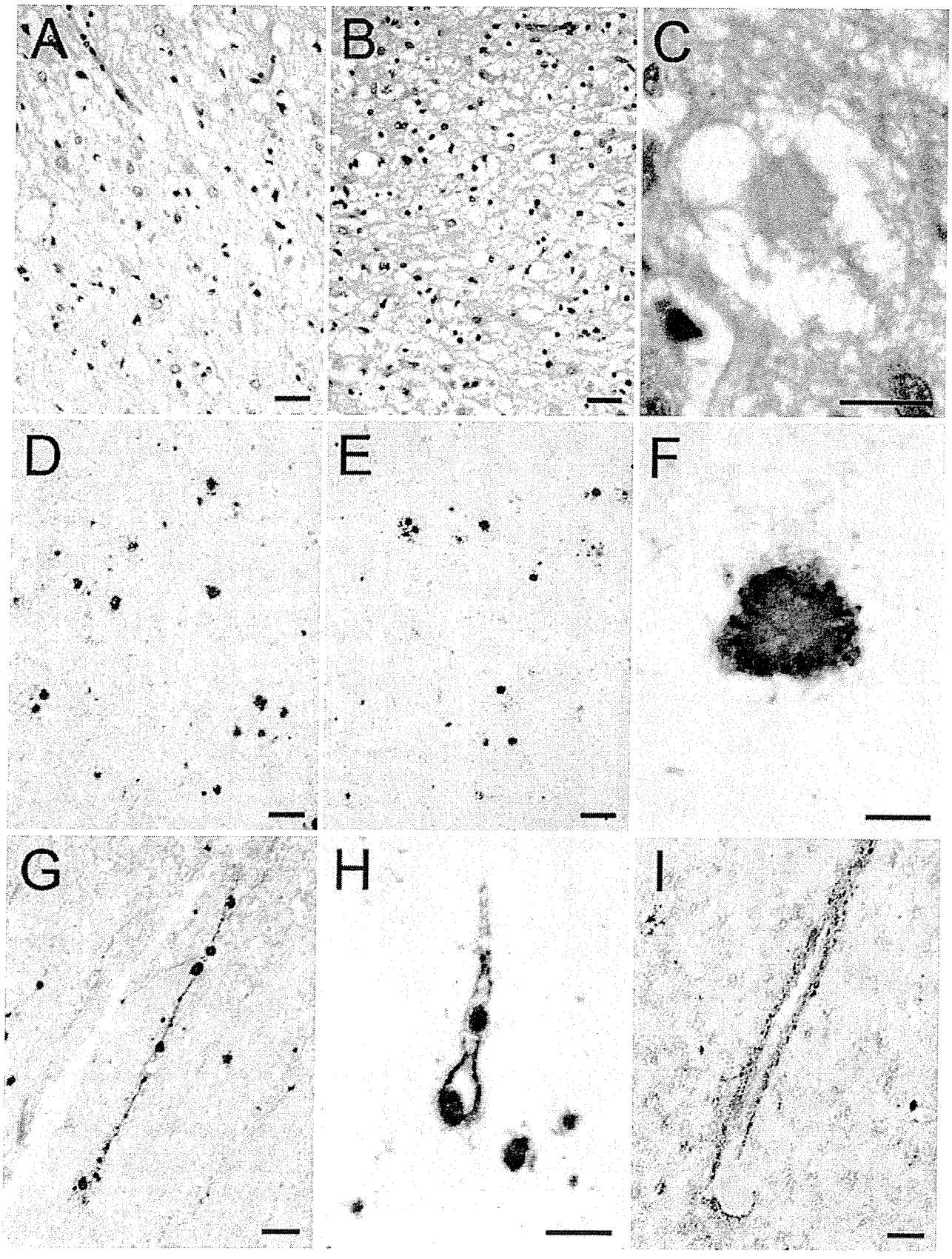

The florid plaques, which are the pathological hallmark of vCJD, are also found in atypical dCJD cases, although they are more abundant in number in vCJD than atypical dCJD cases. These florid plaques distribute widely in the cerebrum and cerebellum but are only occasionally seen in the thalamus in both CJD cases. However, the pathological features of the thalamus are different between these CJD cases. In atypical dCJD cases, spongiform change, neuronal loss and astrocytosis were reported to be intense especially in anterior and medial nuclei.[5] In vCJD cases, while spongiform change is focally seen in anterior and medial thalamic nuclei and pulvinar nuclei are relatively spared from spongiform change, there is extensive neuronal loss with marked astrocytosis in the pulvinar nuclei.[17] In our case, the neuronal loss and astrocytosis were markedly noted in pulvinar nucleus rather than anterior and medial nuclei. Thus, because the pulvinar nucleus of our case presented marked neuronal loss and astrocytosis as well as severe spongiform change and numerous florid plaques, the pathological features of our case was considered to be distinct from those of reported atypical dCJD and vCJD cases.

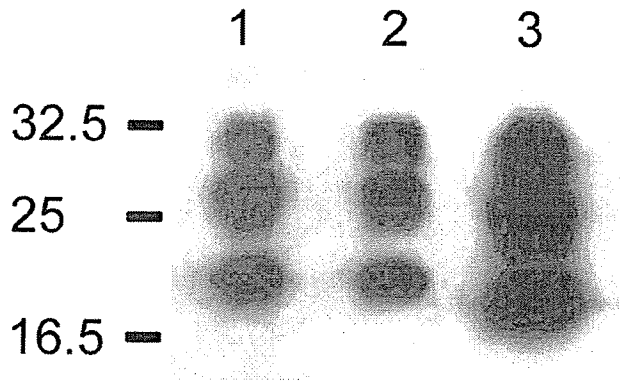

Fig. 3 Immunoblotting. Lane 1, positive control showing type 1 PrP glycoform pattern; lane 2, present study; lane 3, positive control showing type 2 PrP glycoform pattern. The abnormal PrP molecules in the brain homogenates of this case (lane 2) exhibit a type 1 PrP glycoform pattern. Molecular sizes (kDa) are indicated on the left.

Pulvinar increased signals greater than all other basal ganglia on T2-weighted, proton density-weighted, and diffusion-weighted MRI found in our case were unique features and have not been observed in other atypical dCJD cases. The hyperintensity of these images is thought to correlate with the astrocytosis and neuronal loss observed in histological examination.[9] On the other hand, the Gd-DTPA enhancement of the pulvinar nuclei has not been reported in any type of CJD cases. Because the left frontal lesion of the contusion as well as the pulvinar nuclei were enhanced with Gd-DTPA, and because the increased pulvinar signals were asymmetrical and more intense on the left side, these hyperintense signals might reflect damage of the pulvinar nuclei due to a contusion in the left basal forebrain. However, although the thalamus has direct reciprocal connection to the cerebral cortices, the pulvinar nucleus make connections not with the frontal lobe but with the occipital cortex including the striate cortex.[18] In addition, the common pathological findings of the Gd-DTPA-enhancing lesions, the left pulvinar nucleus and the rim of the contusion in the left basal forebrain, was severe astrogliosis. While Gd-DTPA enhancement indicates vascular leakage in general, Gd-DTPA enhancement associated with astrogliosis has also been reported.[19] Therefore, although the precise reason was not clear, we considered that the increased pulvinar signals of our case would reflect pathological changes including severe astrogliosis caused not by traumatic brain injury but by CJD.

The marked pulvinar hyperintensity compared with all other basal ganglia recognized in our case raised the concern of vCJD because the asymmetrical pulvinar hyperintensity has previously been detected in some neuropathologically confirmed vCJD cases.[20] However, the radiological hallmark of vCJD, the pulvinar sign, is defined as symmetrical hyperintensity. Thus, the lack of symmetry in our case was not identical to the radiological features of vCJD cases. In addition, the proposed diagnostic criteria excluded the classification of our case as vCJD after possible iatrogenic exposure.[16] Moreover, the PrP glycoform pattern of our case was type 1 according to Parchi's classification, and was identical to those of reported atypical dCJD cases but was completely different from that of vCJD.[1]

Fig. 2 Verification of abnormal PrP deposition by histological examination. (A–C) HE staining. (D–I) Immunohistochemistry probed with an anti-prion protein antibody (monoclonal, clone 3F4, Senetek, Maryland Heights, MO, USA). Severe spongiform change, neuronal loss, and astrocytosis occurred in the left middle frontal lobe (A) and left pulvinar nucleus of the thalamus (B). (C) A prion protein plaque is surrounded by spongiform changes, to give the appearance of a florid plaque in the pulvinar nucleus. There are many prion plaques in the left middle frontal lobe (D) and in the left pulvinar nucleus of the thalamus (E). (F) The core of the florid plaque is intensely immunostained. (G) Unique prion protein depositions are linearly aligned with the neuronal axon in the left cingulate gyrus. (H) Prion protein deposition occurred around the neuronal cell body and process in the left cingulate gyrus. (I) Granular prion protein deposits are present around the wall of a blood vessel in the left pulvinar nucleus of the thalamus. Bars (A,B,D,E,H) 30 μm, (C,F) 15 μm, (G,I) 60 μm.

Therefore, we concluded our case to be atypical dCJD with radiological and pathological characteristics distinct from those of any dCJD cases.

ACKNOWLEDGMENTS

We thank Ms. K. Hatanaka for her excellent technical assitance.

REFERENCES

1. Satoh K, Muramoto T, Tanaka T *et al.* Association of an 11–12 kDa protease-resistant prion protein fragment with subtypes of dura graft-associated Creutzfeldt-Jakob disease and other prion diseases. *J Gen Virol* 2003; **84**: 2885–2893.
2. Kimura K, Nonaka A, Tashiro H *et al.* Atypical form of dural graft associated Creutzfeldt-Jakob disease: report of a postmortem case with review of the literature. *J Neurol Neurosurg Psychiatry* 2001; **70**: 696–699.
3. Kopp N, Streichenberger N, Deslys JP, Laplanche JL, Chazot G. Creutzfeldt-Jakob disease in a 52-year-old woman with florid plaques. *Lancet* 1996; **348**: 1239–1240.
4. Kretzschmar HA, Sethi S, Földvári Z *et al.* Iatrogenic Creutzfeldt-Jakob disease with florid plaques. *Brain Pathol* 2003; **13**: 245–249.
5. Shimizu S, Hoshi K, Muramoto T *et al.* Creutzfeldt-Jakob disease with florid-type plaques after cadaveric dura mater grafting. *Arch Neurol* 1999; **56**: 357–362.
6. Takashima S, Tateishi J, Taguchi Y, Inoue H. Creutzfeldt-Jakob disease with florid plaques after cadaveric dural graft in a Japanese woman. *Lancet* 1997; **350**: 865–866.
7. Lane KL, Brown P, Howell DN *et al.* Creutzfeldt-Jakob disease in a pregnant woman with an implanted dura mater graft. *Neurosurgery* 1994; **34**: 737–740.
8. Mochizuki Y, Mizutani T, Tahiri N *et al.* Creutzfeldt-Jakob disease with florid plaques after cadaveric dura mater graft. *Neuropathology* 2003; **23**: 136–140.
9. Collie DA, Sellar RJ, Zeidler M, Colchester ACF, Knight R, Will RG. MRI of Creutzfeldt-Jakob disease: imaging features and recommended MRI protocol. *Clin Radiol* 2001; **56**: 726–739.
10. Zeidler M, Sellar RJ, Collie DA *et al.* The pulvinar sign on magnetic resonance imaging in variant Creutzfeldt-Jakob disease. *Lancet* 2000; **355**: 1412–1418.
11. Parchi P, Giese A, Capellari S *et al.* Classification of sporadic Creutzfeldt-Jakob disease based on molecular and phenotypic analysis of 300 subjects. *Ann Neurol* 1999; **46**: 224–233.
12. Santos JMG, Corbalán JAL, Martinez-Lage JF, Guillén JS. CT and MRI in iatrogenic and sporadic Creutzfeldt-Jakob disease: as far as imaging perceives. *Neuroradiology* 1996; **38**: 226–231.
13. Schröter A, Zerr I, Henkel K, Tschampa HJ, Finkenstaedt M, Poser S. Magnetic rosonance imaging in the clinical diagnosis of Creutzfeldt-Jakob disease. *Arch Neurol* 2000; **57**: 1751–1757.
14. Yoon SS, Chan S, Chin S, Lee K, Goodman RR. MRI of Creutzfeldt-Jakob disease: asymmetric high signal intensity of the basal ganglia. *Neurology* 1995; **45**: 1932–1933.
15. Brown P, Preece M, Sato T *et al.* Iatrogenic Creutzfeldt-Jakob disease at the millennium. *Neurology* 2000; **55**: 1075–1081.
16. Will RG, Zeidler M, Stewart GE *et al.* Diagnosis of new variant Creutzfeldt-Jakob disease. *Ann Neurol* 2000; **47**: 575–582.
17. Ironside JW, McCardle L, Horsburgh A *et al.* Pathological diagnosis of variant Creutzfeldt-Jakob disease. *APMIS* 2002; **110**: 79–87.
18. Carpenter MB, Sutin J. Diencephalon. In: Carpenter MB, Sutin J (eds). *Human Neuroanatomy*, 8th edn. Baltimore: Williams & Wilkins, 1983; 500–524.
19. Nishimura R, Takahashi M, Morishita S *et al.* MR Gd-DTPA enhancement of radiation brain injury. *Radiat Med* 1992; **10**: 109–116.
20. Collie DA, Summers DM, Sellar RJ *et al.* Diagnosing variant Creutzfeldt-Jakob disease with the pulvinar sign: MR imaging findings in 86 neuropathologically confirmed cases. *Am J Neuroradiol* 2003; **24**: 1560–1569.

Journal of Pathology
J Pathol 2006; **209**: 484–491
Published online 9 June 2006 in Wiley InterScience
(www.interscience.wiley.com) **DOI:** 10.1002/path.2009

Original Paper

Clusterin expression in follicular dendritic cells associated with prion protein accumulation

K Sasaki,[1]* K Doh-ura,[2] JW Ironside,[3] N Mabbott[4] and T Iwaki[1]

[1]*Department of Neuropathology, Neurological Institute, Graduate School of Medical Sciences, Kyushu University, Fukuoka 812-8582, Japan*
[2]*Division of Prion Biology, Department of Prion Research, CTAAR, Tohoku University School of Medicine, Sendai 980-8575, Japan*
[3]*National CJD Surveillance Unit, University of Edinburgh, Western General Hospital, Edinburgh EH4 2XU, UK*
[4]*Institute for Animal Health, Edinburgh EH9 3JF, UK*

*Correspondence to:
Dr K Sasaki, Department of Neuropathology, Neurological Institute, Graduate School of Medical Sciences, Kyushu University, Fukuoka 812-8582, Japan.
E-mail:
ksasaki@np.med.kyushu-u.ac.jp

Received: 26 January 2006
Revised: 18 March 2006
Accepted: 28 March 2006

Abstract

Peripheral accumulation of abnormal prion protein (PrP) in variant Creutzfeldt–Jakob disease and some animal models of transmissible spongiform encephalopathies (TSEs) may occur in the lymphoreticular system. Within the lymphoid tissues, abnormal PrP accumulation occurs on follicular dendritic cells (FDCs). Clusterin (apolipoprotein J) has been recognized as one of the molecules associated with PrP in TSEs, and clusterin expression is increased in the central nervous system where abnormal PrP deposition has occurred. We therefore examined peripheral clusterin expression in the context of PrP accumulation on FDCs in a range of human and experimental TSEs. PrP was detected immunohistochemically on tissue sections using a novel highly sensitive method involving detergent autoclaving pretreatment. A dendritic network pattern of clusterin immunoreactivity in lymphoid follicles was observed in association with the abnormal PrP on FDCs. The increased clusterin immunoreactivity appeared to correlate with the extent of PrP deposition, irrespective of the pathogen strains, host mouse strains or various immune modifications. The observed co-localization and correlative expression of these proteins suggested that clusterin might be directly associated with abnormal PrP. Indeed, clusterin immunoreactivity in association with PrP was retained after FDC depletion. Together these data suggest that clusterin may act as a chaperone-like molecule for PrP and play an important role in TSE pathogenesis.

Keywords: prion; clusterin; follicular dendritic cell; immunohistochemistry; detergent autoclaving pretreatment; immune deficiency

Introduction

Transmissible spongiform encephalopathy (TSE) is the generic term for the fatal neurodegenerative diseases associated with abnormal prion protein (PrP) deposition in the central nervous system (CNS). Human TSE diseases include Creutzfeldt–Jakob disease (CJD), Gerstmann–Sträussler–Scheinker disease, fatal familial insomnia, and kuru. In cases of variant CJD, transmission is thought to have occurred from exposure to bovine spongiform encephalopathy (BSE)-contaminated meat via the oral route [1–3]. In cases of variant CJD and some animal TSE models, peripheral accumulation of abnormal PrP occurs in the lymphoreticular system, within the lymphoid follicles of spleens, lymph nodes, Peyer's patches, and tonsils [4–6]. In these regions, abnormal PrP accumulates on the surfaces of follicular dendritic cells (FDCs) from an early stage of the disease [7], followed by CNS involvement via the peripheral nervous system [8,9].

Clusterin (apolipoprotein J) is a heterodimeric glycoprotein and is expressed in a variety of mammalian tissues. It is considered to have a variety of functions, including inhibition of complement-mediated cytolysis by binding to the membrane attack complex [10]; regulation of apoptosis [11]; and as a survival factor for germinal centre B cells [12]. We have reported that, during TSE disease, clusterin is associated with deposits of abnormal PrP in the CNS [13]. In the CNS of TSE-affected subjects, clusterin co-localizes with the extracellular plaque-type PrP deposits. Clusterin expression is also up-regulated within lesions of synaptic PrP deposition, even though no co-localization is observed. As clusterin interacts with a range of other molecules [14,15], these findings suggest that secreted clusterin might act as a chaperone-like molecule for PrP. Previous *in vitro* investigations have shown that clusterin is induced in astrocytes by PrP fragments reminiscent of the abnormal PrP isoform [16], and prevents their fibrillar aggregation [17].

FDCs also express clusterin [12]. Therefore we investigated whether clusterin expression in the lymphoreticular system is likewise affected by TSE infection, and associated with the extracellular accumulation of abnormal PrP on FDCs.

Materials and methods

Antibodies

The antibodies used included anti-human PrP C-terminal (rabbit polyclonal, IBL, Japan; raised against a peptide mapping to the C-terminus of human PrP, cross-reacts with mouse PrP), anti-human PrP N-terminal (rabbit, IBL; raised against a peptide mapping to the N-terminus of human PrP, cross-reacts with mouse PrP), anti-human PrP (mouse monoclonal, 3F4, Signet, MA, USA; recognizing amino acid residues 109–112, cross-reacts with hamster PrP), anti-mouse clusterin (goat polyclonal, M-18, Santa Cruz, CA, USA; raised against a peptide mapping to the C-terminus of mouse clusterin), anti-human clusterin (goat, C-18, Santa Cruz; raised against a peptide mapping to the C-terminus of human clusterin), or anti-human clusterin (goat, Chemicon, CA, USA; raised against a purified clusterin from human plasma), anti-mouse CD21/CD35 (CR2/CR1, rat monoclonal, 7G6, PharMingen, CA, USA), anti-human CD35 (CR1, mouse, Ber-MAC-DRC, Dako, Denmark). We assessed two anti-human clusterin antibodies by immunohistochemistry and verified that both gave similar results [13].

Mouse models

Non-transgenic NZW mice and transgenic Tga20 mice [18,19] that express high amounts of mouse PrP were inoculated intraperitoneally (i.p.) with the Fukuoka-1 mouse-passaged scrapie agent strain (NZW/Fu-1, Tga20/Fu-1, respectively). Transgenic Tg7 mice [8,20] that express high amounts of hamster PrP on a mouse-PrP knockout background were inoculated i.p. with the 263K hamster-passaged scrapie agent strain (Tg7/263K). Permission for these animal experiments was obtained from the Animal Experiment Committee of Kyushu University.

Where indicated, C57BL/Dk mice were inoculated either orally or i.p. with the ME7 mouse-passaged scrapie agent strain (C57BL/ME7 mice). To deplete FDCs temporarily, C57BL/Dk mice were given a single i.p. injection of a fusion protein containing the soluble lymphotoxin β receptor domain linked to the Fc portion of human IgG1 (LTβR-Ig) or 100 μg polyclonal human IgG (hu-Ig) (Sandoglobulin®) as a control [21,22]. Where indicated, treatment was given 3 days before (−3 dpi) oral inoculation, or 14 or 42 days after (14 dpi & 42 dpi, respectively) i.p. inoculation with the ME7 scrapie agent strain as described [21,22]. Spleens were analysed 3 days after treatment; Peyer's patches were analysed 70 days after inoculation with the scrapie agent. Mice deficient in interleukin- (IL-) 6 (IL-6-knockout (KO) mice, on a 129/Sv × C57BL/6 background) possess FDC networks but have impaired germinal centres [23]. IL-6-KO mice, and 129/Sv × C57BL/6 immunocompetent wild-type mice, were also inoculated i.p. with the ME7 mouse-passaged scrapie agent strain. Permission for these animal experiments was obtained from the Ethical Review Committee at the Institute for Animal Health, Edinburgh, UK.

Table 1 summarizes the profiles of the mouse lines used in this study.

Human CJD cases

Paraffin-embedded sections of spleens, lymph nodes, appendices, and tonsils were examined from five cases of variant CJD (three males, two females, age range 17–39 years, duration of clinical illness 7–33 months) from the UK National CJD Surveillance Unit, University of Edinburgh, UK. Spleen sections were also examined from four cases of sporadic CJD (two males, two females, age range 55–69 years, duration of clinical illness 4–30 months) from the Department of Neuropathology, Kyushu University. The diagnosis of variant or sporadic CJD was confirmed by postmortem examination. Each case had consent for use of autopsy tissues for research purposes and local Ethics Committee approval for the use of human autopsy tissues from patients with CJD for research was also obtained.

Table 1. Profiles of mouse lines

Line	Background	Modification of PrP expression	PrP^c on FDCs	Reference	Inoculum	PrP^{sc} on FDCs
NZW wild		None	+		Fukuoka-1	+
C57BL/Dk Wild		None	+		ME7	+
Tg7	C57BL/10	MoPrP knockout Overexpress HaPrP under control of the endogenous MoPrP promoter	+	8,20	263K	−
Tga20	129/Sv × C57BL/6	MoPrP knockout Overexpress MoPrP under control of the endogenous MoPrP promoter	−*	18,19	Fukuoka-1	−
IL-6 KO	129/Sv × C57BL/6	None	+	23	ME7	+

MoPrP = mouse PrP; HaPrP = hamster PrP; PrP^c = cellular PrP expression on the FDCs; PrP^{sc} = abnormal PrP accumulation on FDCs of scrapie affected mice; (−) negative; (+) positive.

* Negative on FDCs but some cells within the paracortical T-cell area express PrP^c [19].

The inocula indicated were applied to the respective mouse lines in this study.

J Pathol 2006; **209**: 484–491 DOI: 10.1002/path

Immunohistochemistry

To enhance the detection of PrP by immunohistochemistry (IHC), formalin-fixed, paraffin-embedded sections were pretreated by hydrolytic autoclaving (1–2 mM HCl, 121 °C, 10 min) or a protocol using formic acid, guanidine thiocyanate, and hydrated autoclaving as previously reported [24,25]. We also performed an autoclaving pretreatment with Target Retrieval Solution (Dako) or buffer solution with detergent. A variety of detergents were examined including, Triton X-100 and Tween-20 as non-ionic detergents and sodium dodecyl sulphate as an ionic detergent. We found that non-ionic detergents enhanced PrP detection to a similar degree, whereas the ionic detergent enhanced PrP detection sensitivity, but caused considerable tissue damage. Autoclaving the sections in 0.1% Triton X-100 in 50 mM Tris-HCl, pH 7.6, 121 °C, 20 min, was found to be the most suitable method for the detection of abnormal PrP accumulation on FDCs, and was used in this study (hereinafter referred to as the detergent autoclaving method). Increased concentrations of Triton X-100 up to 0.5% did not significantly increase the signal intensity of the PrP detected or affect the degree of tissue damage. This indicated that the detergent autoclaving method had a wider range of optimum detergent concentrations than the HCl in the hydrolytic autoclaving method. Immunoreactions were visualized using diaminobenzidine as a chromogen.

To examine the co-localization of two different proteins on the same section, the first immunoreaction was visualized using 3-amino-9-ethylcarbazole (AEC; Vector, CA, USA), mapped, and photographed. The section was then decolourized by immersing it in ethanol, and the second immunohistochemical procedure was performed with the other primary antibody. Double immunofluorescence was also performed to reveal sites of co-localization.

Results

Experiments demonstrated that the detergent autoclaving method was the most useful for detecting PrP by IHC. This was particularly evident on sections of spleen tissue, where this method drastically improved the signal intensity for PrP accumulated on FDCs in comparison with sections treated by the HCl autoclave method (Figure 1A and B, respectively). Table 2 shows comparisons between this detergent autoclaving method and conventional techniques for IHC detection of PrP. On human brain samples, most of the different types of PrP deposition could be detected by the detergent autoclaving method as well as by conventional techniques (Figure 1C and 1D, respectively). However, the detergent autoclaving method

Table 2. Comparison of the methods of immunohistochemistry for PrP

	Detergent autoclaving	HCl autoclaving [24]	Three steps [25]
PrP signal intensity			
Synaptic	+ ~ ++	++	+ ~ ++
Plaque	++	++	++
FDCs (mouse)	++	+	++
Background	Low	High	Moderate
Tissue damage	Low	High	Moderate
Simplicity	Simple	Moderate	Complicated

(+) positive; (++) strongly positive.
In the three steps method samples are pretreated with formic acid, guanidine thiocyanate, and hydrated autoclaving.

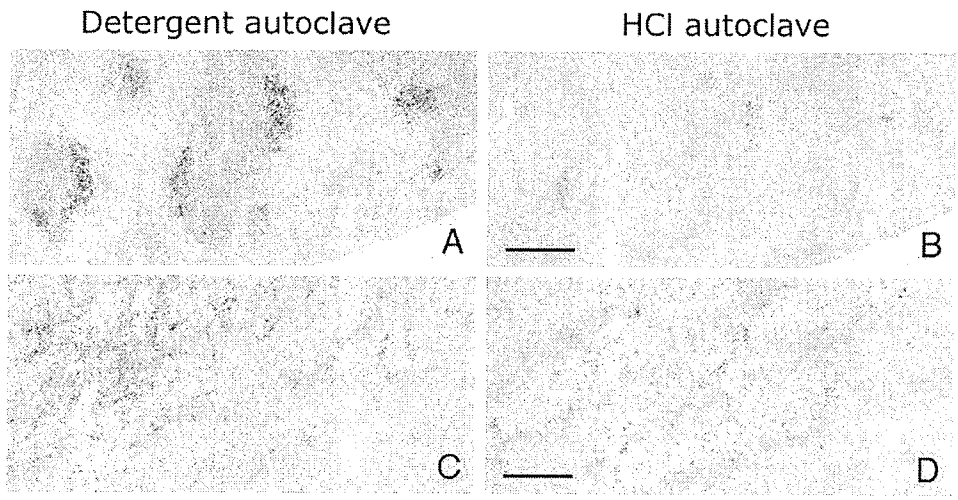

Figure 1. Effect of detergent autoclaving pretreatment on the detection of PrP by immunohistochemistry. (A, B) Serial sections of spleen from TSE-infected mice (NZW mouse inoculated with Fukuoka-1 strain) were immunostained for PrP. The detergent autoclaving method (A) dramatically increased the signal intensity of the PrP immunoreaction and lowered non-specific background staining in comparison with the HCl autoclaving method (B). (C, D) Serial sections of cerebral cortex from a case with sporadic CJD immunostained for PrP. Immunoreactivity for PrP is rather weak on sections pretreated by the detergent autoclaving method (C) in comparison with those pretreated by the HCl autoclaving method (D). However, abnormal fine granular deposits of PrP are detected by both methods. Bars: 200 μm (A, B), 100 μm (C, D)

J Pathol 2006; **209**: 484–491 DOI: 10.1002/path

decreased background staining, which facilitated the double immunofluorescence technique in this study.

We examined the lymphoreticular system of mouse models of TSE. In the spleens of scrapie agent-inoculated NZW/Fu-1 ($n = 5$) and C57BL/ME7 mice ($n = 3$), abnormal PrP accumulated on the dendritic network of FDCs as the disease progressed (Figure 2E), but not in the spleens of uninoculated NZW mice ($n = 5$) (Figure 2B) or scrapie agent-inoculated Tg7/263K ($n = 5$) or Tga20/Fu-1 mice ($n = 3$)(data not shown). The apparent lack of cellular PrP expression by FDCs in the spleens of Tga20 mice probably prevents abnormal PrP amplification on these cells [19]. Likewise, after high-dose scrapie inoculation into these transgenic mice, neuroinvasion probably occurs via a putative 'direct neuroinvasion' pathway without the need for prior amplification of abnormal PrP on FDCs [8]. In uninoculated NZW mice, clusterin was constitutively and diffusely expressed in the reticular cells in lymphoid follicles (Figure 2A), as previously reported [26]. However, in the spleens of NZW/Fu-1 mice immunoreactivity for clusterin was

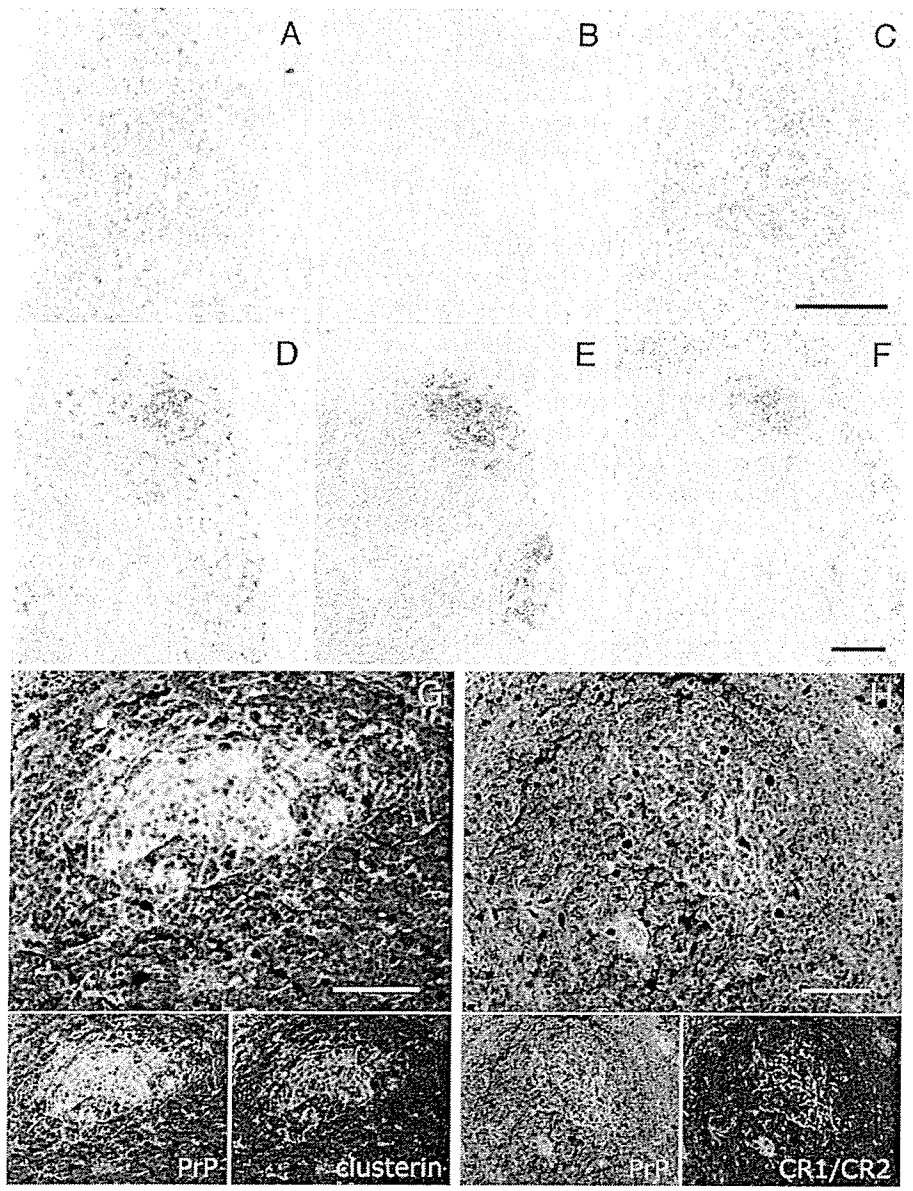

Figure 2. Immunohistochemistry for clusterin expression on FDCs in the spleens of uninoculated and scrapie-inoculated mice. (A–C) Serial sections of uninoculated NZW mouse spleen were immunostained for clusterin (A), PrP (B), and CR1/CR2 (C). Clusterin is constitutively expressed in the reticular cells in the lymphoid follicles of uninoculated mice (A) and not obviously condensed on the dendritic network of FDCs (C). However, increased clusterin expression was observed on FDCs from scrapie-inoculated mice. (D–F) The same section of spleen from the NZW/Fu-1 TSE mouse model was serially immunostained for clusterin (D), PrP (E), and CR1/CR2 (F). Immunoreactivity for clusterin is markedly condensed and increased on the FDCs associated with abnormal PrP accumulation. Similar results were observed in the C57BL/ME7 mouse model. The co-localization of these proteins was also confirmed by double immunofluorescence (G, H). (G) Clusterin (red) and PrP (green). (H) CR1/CR2 (red) and PrP (green). Bars: 100 μm (A–F), 50 μm (G, H)

J Pathol 2006; **209**: 484–491 DOI: 10.1002/path

condensed (Figure 2D) and co-localized with the PrP (Figure 2E) accumulated on the complement receptor 1/2 (CR1/CR2)-immunopositive dendrites [27] of FDCs (Figure 2F). No such accentuation of clusterin expression was observed in the spleens of scrapie-inoculated Tg7/263K mice or Tga20/Fu-1 mice (data not shown). The co-localization of clusterin and PrP on the FDCs was also confirmed by double immunofluorescence (Figure 2G and H).

Although the increased clusterin immunoreactivity mostly correlated with the abnormal PrP accumulations on splenic FDCs from scrapie-agent inoculated C57BL/ME7 mice, temporary FDC depletion 14 or 42 days after scrapie-agent inoculation [21,22] did not affect the association of clusterin with abnormal PrP (Table 3). Similarly, in the spleens of scrapie agent-inoculated IL-6-KO mice, immunoreactivity for clusterin was mostly correlated with abnormal PrP accumulation (Table 3) despite the impaired germinal centre development in these mice [23].

In Peyer's patches, increased clusterin expression was seen not only on the PrP-immunopositive FDCs of infected mice but also in the lymphoid follicles without PrP deposition (Table 3). Clusterin-labelled lymphoid follicles were also confirmed in the Peyer's patches of non-infected control mice (data not shown), but this occurred to a lesser extent than in TSE-infected mice.

Increased clusterin expression associated with the abnormal PrP deposition on FDCs was also observed in cases of human variant CJD. The extent and intensity of clusterin immunoreactivity did not appear to be related to the age of the patient, or the duration of the clinical illness of the five cases examined (patient ages 17, 29, 33, 36, and 39 years; duration of clinical illness 33, 7, 18, 15, and 14 months, respectively). In each case, immunoreactivity for clusterin was increased wherever abnormal PrP accumulation on the FDCs was found, such as in the spleens, lymph nodes, appendices, and tonsils (Figure 3). In appendices, clusterin immunoreactivity was also increased in the lymphoid follicles without PrP deposition (Figure 3C and D), which was consistent with data from analysis of Peyer's patches of mouse TSE models. No increased clusterin immunoreactivity was observed on FDCs from sporadic CJD cases (data not shown) in which no PrP deposition was detected, except on appendices where clusterin immunoreactivity was increased on the FDCs even in non-CJD control cases (Figure 3E and F).

Discussion

Here we show that clusterin expression on FDCs is increased during TSE diseases and occurs in association with abnormal PrP accumulation. The dendritic network pattern of the clusterin immunoreactivity in the lymphoid follicles was associated with PrP accumulation on FDCs in NZW/Fu-1 mice and C57BL/ME7 mice. The increased clusterin immunoreactivity was mostly dependent on the presence of

Table 3. Effect of FDC depletion and impaired germinal centre development on clusterin expression in TSE-inoculated mice

	Immune deficiency	PrP IR	Clusterin IR*	CR1/CR2 IR	Effect on disease transmission†
Spleens					***Intraperitoneal***
Uninfected					
LTβR-Ig	FDCs depleted	−	−	−	n/a
Hu-Ig	Control	−	−	+	n/a
14 dpi					
LTβR-Ig	FDCs depleted	−	−	−	Delayed [21]
Hu-Ig	Control	+−	−	+	
42 dpi					
LTβR-Ig	FDCs depleted	+	+	−	Delayed [21]
Hu-Ig	Control	+	+	++	
IL-6-KO	Impaired germinal centres	++	+	++	No effect [23]
Wild-type	Control	++	+	++	
Peyer's patches					***Oral***
−3 dpi					
LTβR-Ig	FDCs depleted	−	+‡	n.d.	Inhibited [22]
Hu-Ig	Control	+	+‡	n.d.	

FDCs were depleted by treatment with LTβR-Ig, or Hu-Ig as a control [28]. Ig treatment was performed on the indicated days relative to scrapie challenge. Three mice were examined and estimated the immunoreactivity on each immune-deficient group (LTβR-Ig treated or IL-6 KO) or control group.

IR = immunoreactivity; dpi = days post scrapie inoculation; n.d. = not determined; n/a = not applicable; (−) = negative; (+−) = faint; (+) = positive; (++) = strongly positive.

* Immunoreactivity in the dendritic-network pattern.

† Data from previous reports [21–23].

‡ Clusterin immunoreactivity does not always correlate with PrP deposition; increased clusterin expression is also seen in some lymphoid follicles without PrP accumulation.

J Pathol 2006; **209**: 484–491 DOI: 10.1002/path

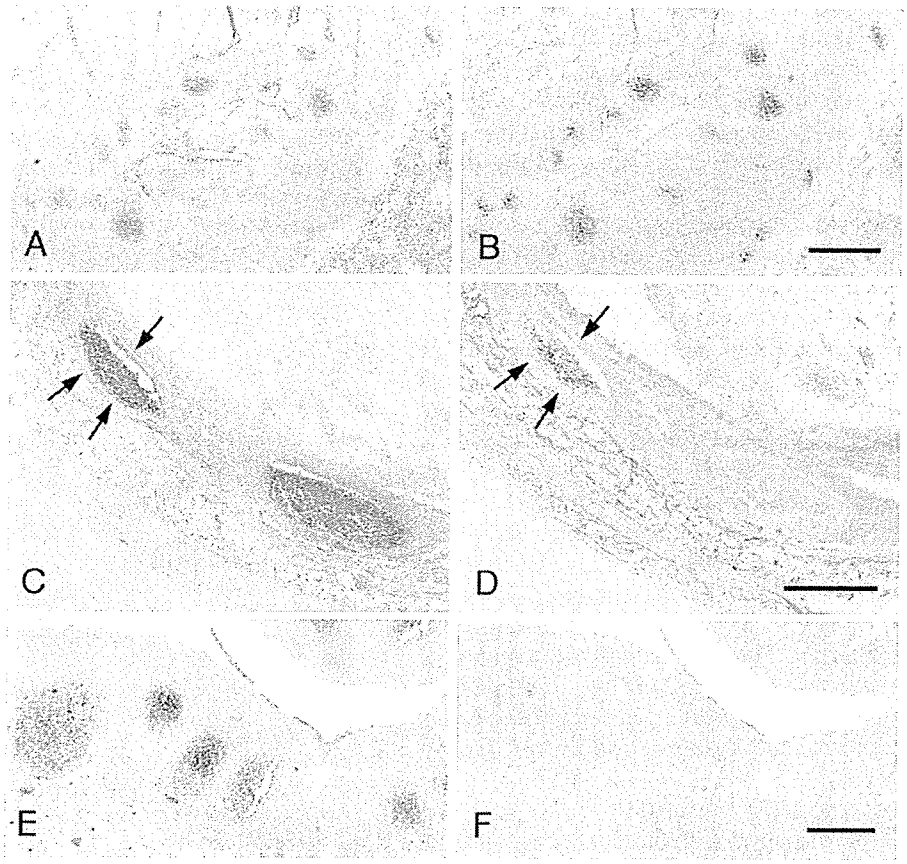

Figure 3. Immunohistochemistry of lymphoreticular tissues from human variant CJD and control (non-CJD) cases. (A, C, E) Clusterin. (B, D, F) PrP. (A, B) Serial sections of the tonsil from a variant CJD case. Clusterin immunoreactivity is increased on FDCs where abnormal PrP deposits are detected. (C–F) Serial sections of appendices from a variant CJD case (C, D) and a control case (E, F). Note that not only the lymphoid follicles with PrP accumulation (arrows) but also those without PrP accumulation show increased clusterin expression. Bars: 500 μm

abnormal PrP deposition, irrespective of the TSE agent strains, host mouse strains, or various immune deficiencies. Moreover, clusterin accumulation was also seen in human variant CJD cases, which was consistently accompanied by PrP deposition on FDCs in the lymphoreticular system (except for the intestinal lymphoid follicles). We have previously reported that clusterin expression in the cerebrum was increased in association with increased PrP deposition [13]. The results in the present report provide evidence that clusterin accumulation also occurs in peripheral lymphoid tissues. Although a direct interaction between clusterin and PrP remains to be confirmed, these data suggest that clusterin may play an important role in the pathogenesis of TSE diseases in lymphoid tissues.

To determine whether clusterin was associated with abnormal PrP, we analysed the effect of FDC depletion on clusterin accumulation. Signalling through the LTβR provides important stimuli for FDC maturation and maintenance. Blockade of this stimulation through treatment with LTβR-Ig causes the temporary de-differentiation of FDCs [28]. In this study, CR1/CR2 expression on FDCs was certainly affected by LTβR-Ig treatment in comparison with the control mice treated with Hu-Ig (Table 3), confirming that the FDCs were temporarily de-differentiated. In uninoculated mice, clusterin expression by FDCs is down-regulated by LTβR signalling blockade and undetectable by immunohistochemistry within two days of FDC depletion [12]. However, in this study we show that the detection of clusterin in the spleens of scrapie-inoculated mice was unaffected by FDC depletion and remained in close association with abnormal PrP (Table 3). These data imply that clusterin associates directly with abnormal PrP molecules exposed extracellularly on the surface of FDC dendrites.

Why clusterin expression is up-regulated during TSE disease is not known. Data from both human and experimental studies demonstrate that TSE infections induce the expression of both early and terminal complement components within the brain. However, the membrane attack complex (C5b–C9) is not involved in TSE pathogenesis [29]. Thus it is plausible that, during TSE diseases within the CNS, clusterin might be expressed as part of an innate response to inactivate the membrane attack complex formed by the terminal complement components [10], and to help protect neurons from potential complement-mediated lysis. It is also plausible that clusterin might be induced to exert anti-amyloidogenic properties [30]. Because